Seismic Design and Buckling Strength Evaluation of Liquid-Filled Steel Cylindrical Tanks

Wiriyachai Roopkumdee
University of North Dakota
wiriyachai.roopkumde@und.edu

Iraj Mamaghani
University of North Dakota
iraj.mamaghani@engr.und.edu

Abstract

This paper describes the development of a practical seismic design equation to estimate the buckling strength of liquid-filled cylindrical tanks subjected to earthquake loads. A pseudo-equilibrium path criterion is used to evaluate buckling strength. Finite element analysis is performed using ANSYS computer program. The modeling method, appropriate element types, and necessary number of elements to use in numerical analysis are recommended.

Characteristics of earthquake excitations play an important role in the buckling strength of liquid-filled steel cylindrical tanks. Based on the extensive parametric study, seismic design equations and design curves representing the interactions of D/t and H/D ratios for the cylindrical tanks of various geometries subjected to El Centro 1940, Parkfield 2004, and Northridge 1994 earthquakes are presented and discussed. Results revealed that the D/t ratio is an important parametric factor of the seismic buckling strength of the liquid-filled cylindrical tank. The dynamic buckling capacity of the tank decreases significantly when the D/t ratio increases. An increase in H/D ratio also seems to have a negative effect on the seismic buckling strength; however, its effect is less significant compared to the D/t ratio.

Introduction

Liquid storage tanks are subjected to the horizontal and vertical ground accelerations during the earthquakes. Damage to petroleum storage tanks was reported due to several earthquakes: 1933 Long Beach, 1952 Kern County, 1964 Alaska, 1971 San Fernando, 1979 Imperial Valley, 1983 Coalinga, 1989 Loma Prieta, 1992 Landers, 1994 Northridge, and 1995 Kobe (Cooper & Wachholz, 1999). The American Lifelines Alliance (2005) reported the failure modes occurred due to steel storage tanks. This study explores the shell buckling mode of liquid-filled cylindrical tanks subjected to the horizontal earthquake accelerations. The hydrodynamic behavior of liquid-filled cylindrical tanks when the cylindrical tanks are subjected to the earthquakes can be distinguished into two types (Housner, 1963): impulsive mass, where a mass of water is rigidly attached to the tank at the proper height; and convective mass, when horizontal accelerations from the tank excite a mass of water into oscillations. Veletsos and Yang (1977) reported that liquid contained cylindrical tanks have a

cantilever beam mode when the tanks are subjected to horizontal excitation. Housner (1963), Haroun and Housner (1981), and Veletsos and Yang (1977) reported that when horizontal excitations were applied to a liquid-filled cylindrical tank, a cantilever-beam mode was detected. From past earthquakes, recorded data have shown that tanks filled with liquid are more prone to suffer damage (American, 2005).

Sezen et al. (2008) used an ANSYS computer program to study liquefied gas-structure interaction and a simplified model of three tanks in Turkey that experienced an earthquake on August 17, 1999; they reported that shear and bending moments are overestimated if the fluid is modeled as a single rigid mass. Virella et al. (2006) presented the critical value of peak ground acceleration (PGA) for conical roof tanks subject to horizontal acceleration, using ABAQUS finite element analysis software, the critical values of PGA for cylindrical tanks filled with liquid up to 90% of the tanks' height are between 0.25g and 0.35g. The nature of the dynamic buckling response can be estimated using the deformations and stresses around the critical level of the earthquake excitation (Djermane, Zaoui, Labbaci, & Hammadi, 2014).

Djermane et al. (2014) and Virella et al. (2006) used Budiansky and Roth (1962) to conduct the pseudo-equilibrium path to find a significant increase rate of the deformation. This significant increase rate of deformation can be used to indicate the dynamic buckling of the steel cylindrical tanks. Kazaz et al. (2006) conducted the numerical simulation of reinforced concrete load-bearing structural wall model subjected to effective earthquake forces.

Many research studies have examined the seismic behavior of liquid-filled steel cylindrical tanks. However, little effort has been devoted to investigating the interaction effects of D/t and H/D ratios on seismic buckling capacities when liquid-filled steel cylindrical tanks are subjected to different earthquake excitations.

In this study, the finite element method (FEM) was used to investigate the effects of D/t and H/D ratios of the liquid-filled steel cylindrical tanks when different characteristics of earthquake loads are applied to the tanks. The structure response to the base excitation was modeled using the concept of effective earthquake forces; therefore, acceleration input was to create acceleration fields acting on all the nodes of the model. In addition, the time steps were divided to be small enough to accurately capture the periods of oscillations.

Modeling of Cylindrical Tanks

Five different geometric configurations of the cylindrical tanks are analyzed with height-to-diameter (H/D) ratios of 0.43, 0.67, 1.00, 1.46, and 2.41 and the diameter-to-thickness (D/t) ratios of 910, 1013, 1216, 1612, and 2130 to investigate the buckling behaviors of various sizes of the cylindrical tanks. The geometries of the cylindrical tanks are illustrated in Table 1 and Figure 1. FEA modeling of model A is illustrated in Figure 2.

Table 1. Geometries of the cylindrical tanks.

Model	H (m)	D (m)	t (mm)	Hr (m)	H/D	D/t
A	6.1	9.1	10.0	0.853	0.67	910
B	18.3	7.6	7.5	0.713	2.41	1013
C	15.2	15.2	12.5	1.425	1.00	1216
D	20.0	13.7	8.5	1.284	1.46	1612
E	9.1	21.3	10.0	2.000	0.43	2130

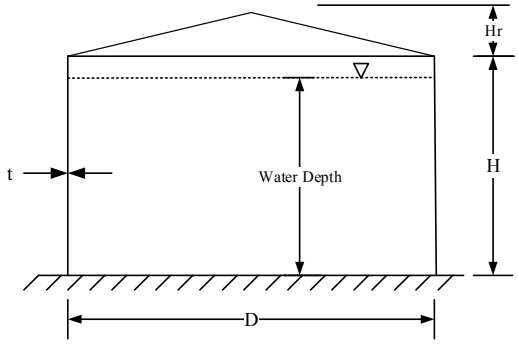

*Figure 1***.** Cylindrical tank geometry.

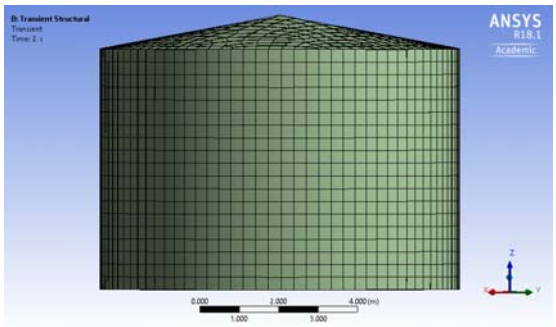

Figure 2. FEA modeling of model A.

The material for all cylindrical storage tanks is steel with a modulus of elasticity, E = 200GPa, Poisson's ratio, ν = 0.3, and mass density of ρ = 7,850kg/m^3. Bilinear isotropic hardening of the steel is included with the yield stress of 345MPa and the tangent modulus of 13.79 GPa. The liquid inside the tanks is water, with a bulk modulus of 2,068.4MPa and a mass density of 1,000kg/m^3.

For FEA modeling, all cylindrical tanks are considered fixed at the base and free on the top. The histogram of earthquake excitation in terms of acceleration is applied to every node of cylindrical tanks. Therefore, the structural response to the base excitation was modeled using the concept of effective earthquake forces (Chopra, 2011), as illustrated in Figure 3.

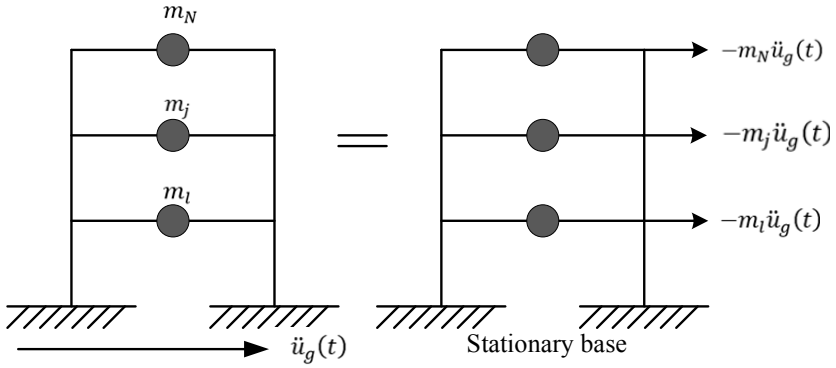

Figure 3. Ground excitation and effective earthquake forces

The ANSYS computer program was used for all computations. SHELL181 element was used for the steel cylindrical tanks. SOLID186 element was used as the element for the water inside the tanks. SHELL181 is a four-node element with six degrees of freedom at each node (translation in x, y, and z directions, and rotation about x, y, and z axes). SOLID186 is a higher order 3-D 20-node having three degrees of freedom per node solid element that exhibits quadratic displacement behavior (ANSYS, 2009). The elements of SHELL181 for models A, B, C, D, and E were modeled with 4174, 5513, 8838, 7941, and 7198 elements, respectively. The elements of SOLID186 for model A, B, C, D, and E were modeled with 850, 941, 1180, 1021, and 978 elements, respectively.

Damping Ratios

Rayleigh damping is a procedure of classical damping, which is used in the ANSYS computer program. For simplicity and numerical efficiency, the damping is assumed as Rayleigh mass proportional damping as Equation 1 and Equation 2

$$[C] = a_0[M] \tag{1}$$

$$a_0 = 2\omega_n\zeta_n \tag{2}$$

where a_0 is mass coefficient, and ζ_n is critical damping ratio.

For the steel structure, the critical damping ratio is generally between 2% and 3% (Djermane et al., 2014). This study adopts the value of 2%. This mass coefficient (a_0) is input into the transient analysis to indicate the damping ratio of the structure. The mass coefficients of each model are represented in Table 2.

Table 2. First natural frequencies and mass coefficients of tanks filled with water up to 90% height.

Model	First Natural Frequency (Hz)	Mass Coefficient (a_0)
A	4.259	0.17034
B	1.993	0.07974
C	2.293	0.09173
D	1.824	0.07296
E	2.070	0.08280

Nonlinear Seismic Analysis

The transient dynamic analysis can be used in FEM to study the dynamic behavior of a structure when it is subjected to a time-dependent loading. Inertia and damping effects are considered for the transient dynamic analysis. The equation of motion, Equation 3, is solved by the transient structure simulation in the ANSYS computer program.

$$[M]\{\ddot{u}\} + [C]\{\dot{u}\} + [K]\{u\} = \{F_{(t)}\} \tag{3}$$

where $[M]$ is mass matrix, $[C]$ is damping matrix, $[K]$ is stiffness matrix, $\{\ddot{u}\}$ is nodal acceleration vector, $\{\dot{u}\}$ is nodal velocity vector, $\{u\}$ is nodal displacement, $\{F_{(t)}\}$ is load vector, and t is time.

Data sets of earthquake loads of El Centro 1940, Parkfield 2004, and Northridge 1994 were collected from the United States Geological Survey (Index, 2014). Numerical values of these earthquakes are in the unit of g, the accelerations due to gravity for the El Centro, Parkfield, and Northridge earthquakes are presented in Figures 4, 5, and 6, respectively.

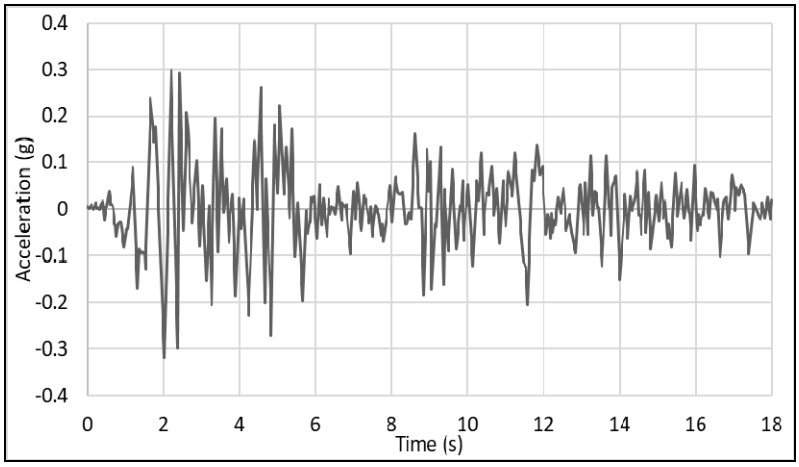

Figure 4. Accelerogram of north-south component of El Centro earthquake, 1940.

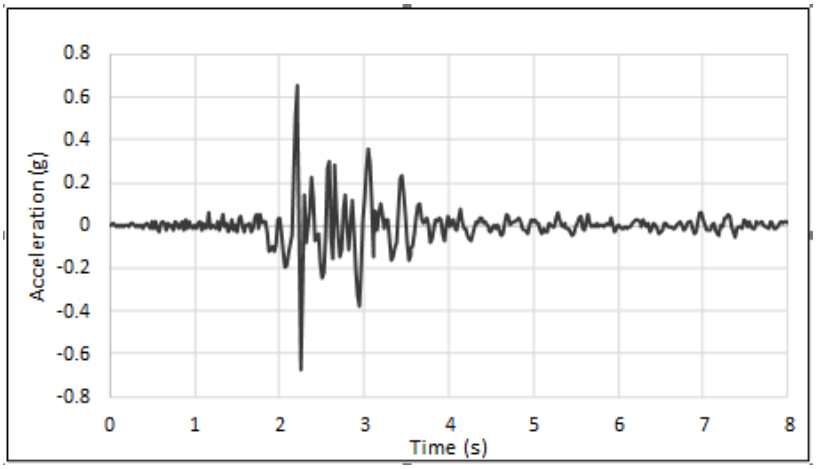

Figure 5. Accelerogram of north-south component of Parkfield earthquake, 2004.

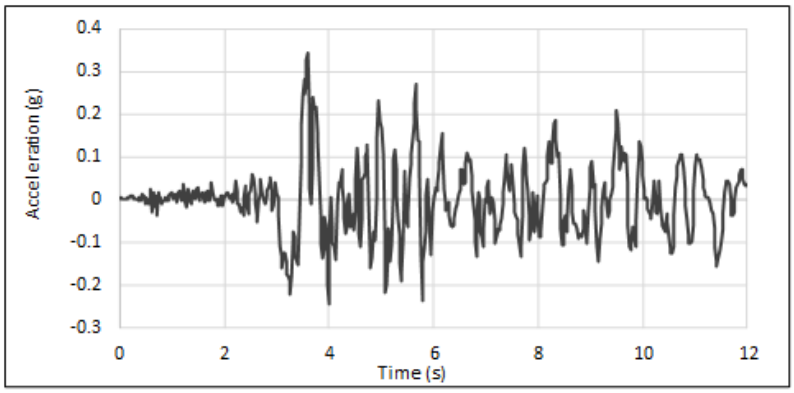

Figure 6. Accelerogram of north-south component of Northridge earthquake, 1994.

Pseudo-Equilibrium Paths

El Centro Earthquake

The Budiansky and Roth criterion (1962) was used to generate pseudo-equilibrium paths in this study. Buckling instability occurs when a small increase in pulse intensity causes a strong increase rate of the deflection. Therefore, different analyses of the structure for several loads (PGAs) must be constructed. The node that gave the maximum displacement of each model was used to find the pseudo-equilibrium path. For example, node 2638 has a maximum displacement when PGA is 0.7g, as illustrated in Figure 7. Figure 8 shows the pseudo-equilibrium paths and the dynamic buckling values of models A and C. The dynamic buckling values of model A and C are 0.72g and 0.56g, respectively. Figure 9 illustrates the pseudo-equilibrium paths and the dynamic buckling value of model B (0.55g). Figure 10 shows the pseudo-equilibrium paths and the dynamic buckling values of models D and E, 0.15g and 0.075g, respectively.

This study also observed transient response curves in terms of nodal displacement with an increase in PGA. Figure 11 shows the significant jump in the nodal displacement of model C, which indicates that the structure is unstable for PGA = 0.6g.

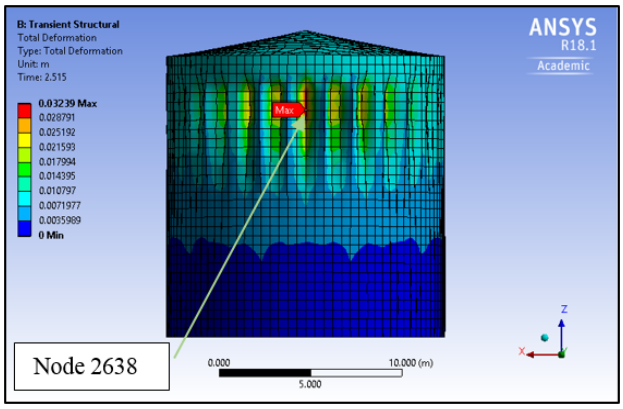

Figure 7. Deformation of model C subjected to El Centro earthquake.

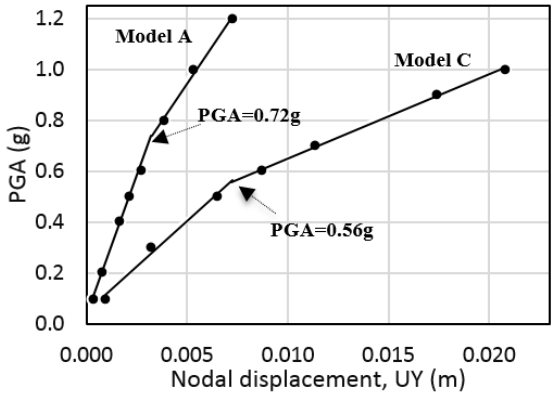

Figure 8. Pseudo-equilibrium paths for model A and C.

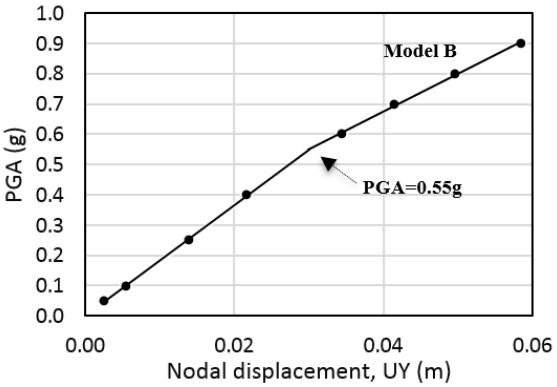

Figure 9. Pseudo-equilibrium path for model B.

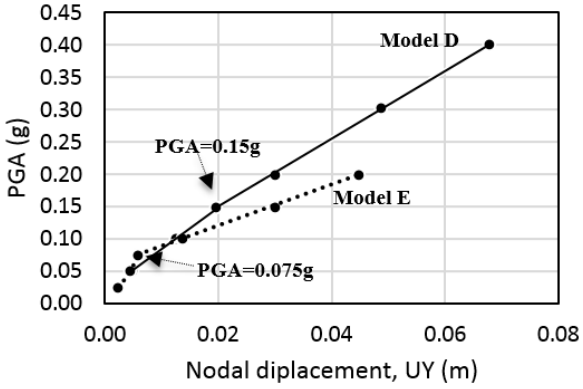

Figure 10. Pseudo-equilibrium paths for model D and E.

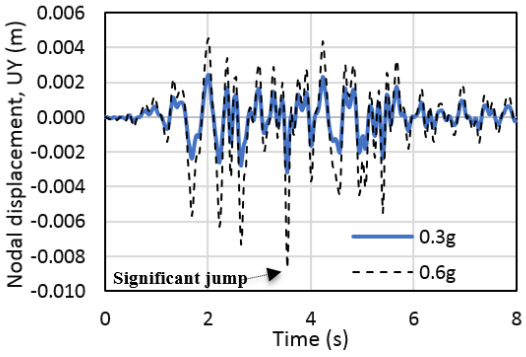

Figure 11. Transient response for model C.

Parkfield Earthquake

The Parkfield earthquake was chosen to illustrate the dynamic buckling strength of liquid-filled steel cylindrical tanks when different characteristics of earthquake load were applied to the tanks. Nodes that gave the maximum displacement to the tanks subjected to the Parkfield earthquake are nodes 2623, 2876, 5580, 1076, and 1436 for models A, B, C, D, and E, respectively. Figure 12 illustrates the pseudo-equilibrium path and the dynamic buckling value of model A (1.30g), while Figure 13 shows the pseudo-equilibrium paths and the dynamic buckling values of model C and D, 0.88g and 0.40g, respectively. The pseudo-equilibrium path and the dynamic buckling value of model B is illustrated in Figure 14, 1.20g. Figure 15 presents the pseudo-equilibrium path and the dynamic buckling value of model E, 0.33g.

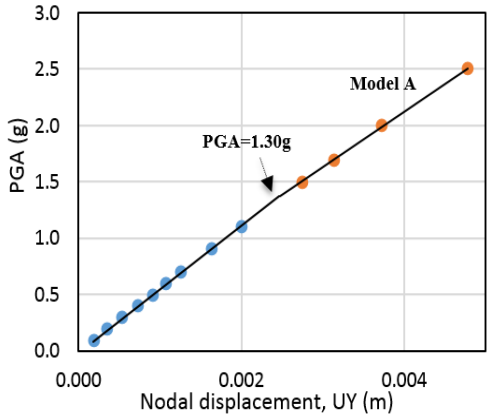

Figure 12. Pseudo-equilibrium path for model A.

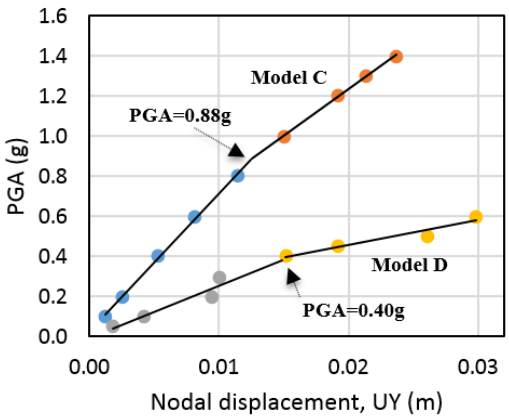

Figure 13. Pseudo-equilibrium paths for model C and D.

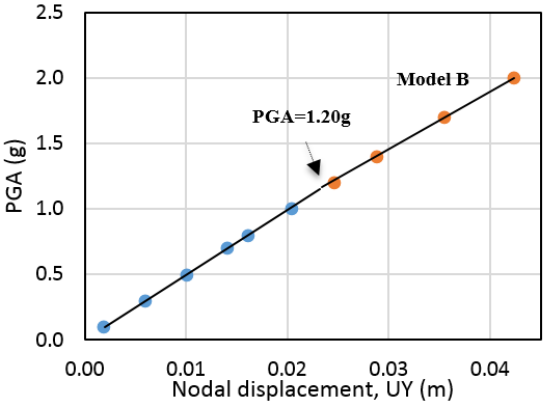

Figure 14. Pseudo-equilibrium path for model B.

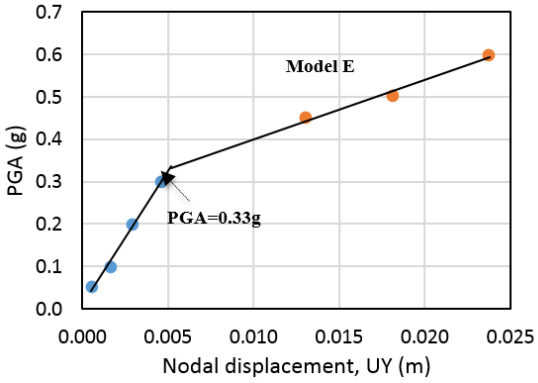

Figure 15. Pseudo-equilibrium path for model E.

Northridge Earthquake

The results of finite element models using El Centro and Parkfield earthquakes indicate that the dynamic buckling capacities decrease when D/t ratios increase; however, the effect of H/D ratio could not be simplified. Thus, the Northridge earthquake was included in this study to interpret the H/D ratio's uncertain effect. Figure 16 illustrates the pseudo-equilibrium paths and the dynamic buckling values of model A and C, which are 1.34g and 0.70g, respectively. Figure 17 illustrates the pseudo-equilibrium path and the dynamic buckling value of model B, 0.63g, and Figure 18 presents the pseudo-equilibrium paths and the dynamic buckling values of models D and E, 0.21g and 0.20g, respectively. Figure 19 shows the significant jumps from transient response curves for model D.

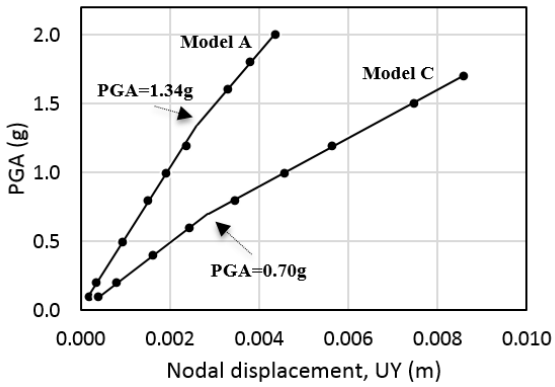

Figure 16. Pseudo-equilibrium paths for model A and C.

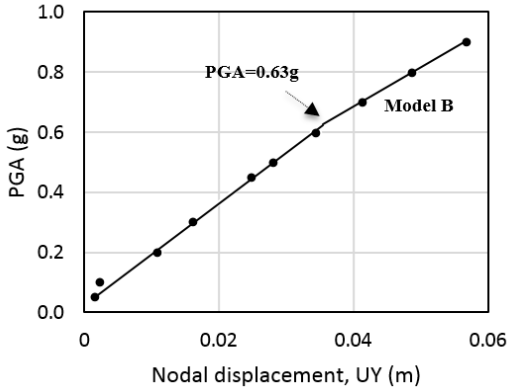

Figure 17. Pseudo-equilibrium path for model B.

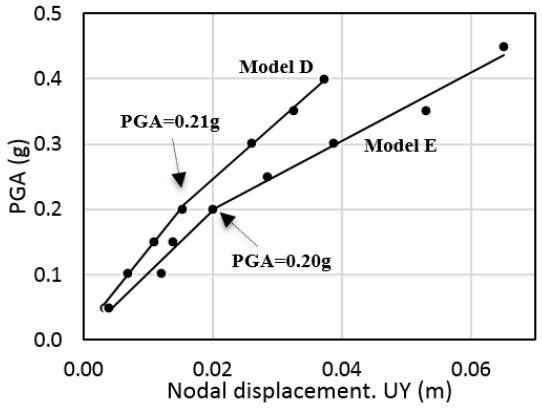

Figure 18. Pseudo-equilibrium paths for model D and E.

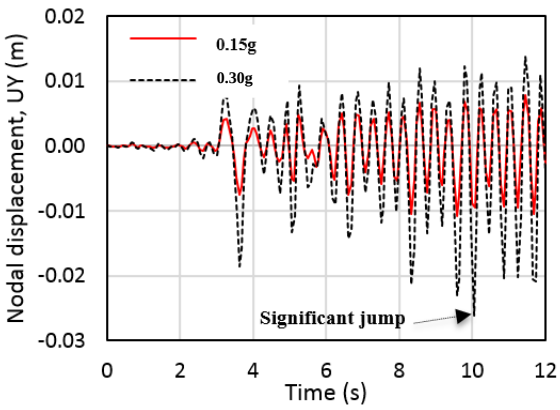

Figure 19. Transient response for model D.

Estimated Design Equation

To estimate the interaction effects of H/D and D/t ratios on the seismic buckling strengths of the steel cylindrical tanks, nonlinear regression analysis was adopted to estimate a design equation. From the El Centro, Parkfield, and Northridge earthquake cases, a design equation can be estimated as Equation 10.

$$PGA = -0.28375\ln(H/D) - 2.93(10^{-7})(D/t)^2 + 1.23015;\ R^2 = 0.7018 \quad (4)$$

From Equation 10, D/t ratio has a significant negative effect on the dynamic buckling capacity. If D/t ratio increases, the dynamic buckling capacity will significantly decrease. An increase in H/D ratio also shows a negative effect on dynamic buckling capacity; however, when H/D ratio increases, the buckling capacities will decrease with a diminishing rate. Equation 10 was estimated from geometries of the tanks based on this study. Therefore, the estimated design equation may need reinvestigation if the tank dimensions are not included in this study.

Conclusion

This paper evaluated the seismic buckling capacities of liquid-filled steel cylindrical tanks of various sizes. The interaction effects of D/t and H/D ratios on dynamic buckling were investigated, and estimated design equations were proposed. Results show that the D/t ratio is an important parametric factor of the seismic buckling strength of a liquid-filled cylindrical tank. The dynamic buckling capacity of the tank decreases significantly when the D/t ratio increases. An increase in H/D ratio also seems to have a negative effect on the seismic buckling strength; however, its effect is less significant compared to the D/t ratio.

References

American Lifelines Alliance. (2005, March). *Seismic guidelines for water pipelines*. Retrieved from https://www.americanlifelinesalliance.com/pdf/SeismicGuidelines_WaterPipelines_P3.pdf

ANSYS, Inc. (2009). *ANSYS training manual*. Canonsburg, PA: Ansys.

Budiansky, B., & Roth, R. S. (1962). Axisymmetric dynamic buckling of clamped shallow spherical shells. *Proceedings of the 11th International Congress of Applied Mechanics*. Munich: Springer-Verlag.

Chopra, A. K. (2011). *Dynamics of structures: Theory and application to earthquake engineering*. (4th ed.). Upper Saddle River, NJ: Prentice Hall.

Cooper, T. W., & Wachholz, T. P. (1999). Optimizing post-earthquake lifeline system reliability. *Proceedings of the 5th US Conference on Lifeline Earthquake Engineering*. Reston, VA: ASCE.

Djermane, M., Zaoui, D., Labbaci, B., & Hammadi, F. (2014). Dynamic buckling of steel tanks under seismic excitation: Numerical evaluation of code provisions. *Engineering Structures*, *70*, 181-196.

Haroun, M. A., & Housner, G. W. (1981). Earthquake response of deformable liquid storage tanks. *Journal of Applied Mechanics*, *48*(2), 411-418.
Housner, G. W. (1963). The dynamic behavior of water tanks. *Bulletin of the Seismological society of America*, *53*(2), 381-387.
Index to NSMP data sets. (2014, March 19). Retrieved from https://escweb.wr.usgs.gov/nsmp-data/
Kazaz, İ., Yakut, A., & Gülkan, P. (2006). Numerical simulation of dynamic shear wall tests: a benchmark study. *Computers & Structures*, *84*(8-9), 549-562.
Sezen, H., Livaoglu, R., & Dogangun, A. (2008). Dynamic analysis and seismic performance evaluation of above-ground liquid-containing tanks. *Engineering Structures*, *30*(3), 794-803.
Veletsos, A. S., & Yang, J. (1977). Earthquake response of liquid storage tanks. *Proceedings of the Second Engineering Mechanics Specialty Conference*. Reston, VA: ASCE.
Virella, J. C., Godoy, L. A., & Suárez, L. E. (2006). Dynamic buckling of anchored steel tanks subjected to horizontal earthquake excitation. *Journal of Constructional Steel Research*, *62*(6), 521-531.

Biographies

WIRIYACHAI ROOPKUMDEE is currently a PhD student of Civil Engineering Department at the University of North Dakota. Wiriyachai Roopkumdee may be reached at wiriyachai.roopkumde@und.edu.

IRAJ H. P. MAMAGHANI is an associate professor of Civil Engineering at University of North Dakota. He received his BSc in Civil Engineering from Istanbul Technical University, with 1st Class Honors, in 1989. He continued his master's and PhD studies at University of Nagoya, Japan, where he obtained his master's and Doctor of Engineering degrees in Civil Engineering. Dr. Mamaghani works in civil engineering, with an emphasis on structural mechanics and structural engineering. He focuses on cyclic elastoplastic material modeling, structural stability, seismic design, advanced finite element analysis and ductility evaluation of steel, composite (concrete-filled steel tubular), and masonry structures. Dr. Mamaghani may be reached at iraj.mamaghani@engr.und.edu.